Quantification of Image Distortion of Orthopedic Materials in Magnetic Resonance Imaging

Matthew F Koff[1], Parina Shah[1], Kevin M Koch[2], and Hollis G Potter[1]

[1]*Department of Radiology and Imaging - MRI, Hospital for Special Surgery, New York, New York, United States,* [2]*Applied Science Laboratory, General Electric Healthcare, Waukesha, Wisconsin, United States*

Introduction. Magnetic resonance imaging (MRI) of anatomy surrounding orthopedic materials is difficult due to metal susceptibility artifact which produces in-plane and through-plane image distortions. The generated images are distorted and "pixel-pileup" limits the visualization of the bone-implant interface. The multi-acquisition variable-resonance image combination (MAVRIC) technique has recently been shown to minimize image distortions by combining image datasets acquired at numerous frequency bands offset from the dominant proton frequency (1,2). Currently, the amount of artifact reduction by MAVRIC compared to a metal specific fast-spin-echo (FSE) protocol is unknown. The goal of this study was to determine the magnitude of in-plane image distortion between standard of care 2D fast-spin-echo (FSE) images and corresponding MAVRIC images. This was accomplished by using a novel MRI phantom which allows for placement of material samples frequently used in total joint replacements.

Methods. A custom phantom, composed of a series of grids, was manufactured from polycarbonate. The phantom was designed to hold small prismatic bars of known dimensions of common orthopedic materials: Stainless Steel 316, Cobalt Chrome, Titanium, and ultra-high molecular weight polyethylene (UHMWPE). *Imaging Protocol*: All images were acquired in a clinical 1.5T scanner using an 8 channel cardiac phased array coil (General Electric, Waukesha, WI). Initial axial and coronal FSE images were acquired iteratively to modify the position of the phantom and ensure alignment of the phantom with the bore of the scanner, orthogonal to B_o. 2D-FSE images were acquired: TE: 23ms, TR: 3500ms, ETL: 21, NEX: 4, matrix: 512x256, FOV: 24cm, slice thickness: 3mm, RBW: ±125kHz. 3D-MAVRIC images, with the same voxel size and at identical slice locations of the 2D-FSE images were also acquired: TE: 40ms, TR: 4000ms, ETL: 24, NEX: 0.5, RBW: ±125kHz. The voxel dimensions for all scans was 0.468mm x 0.468mm x 3mm. A duplicate set of 2D-FSE and 3D-MAVRIC images were acquired to assess measurement repeatability. In addition, image acquisition was repeated with no material samples (Control) within the phantom. *Image Analysis*: A custom semi-automated program (Matlab, Natick, MA) detected all corners in the image which were then localized to the constructed grid. The 3D coordinates of these corners were calculated from the DICOM header information. The 3D displacement between a point on the MAVRIC scan and the same point on the FSE scan was calculated. Results are reported for all corners on the grid, and for corners in 3 subregions defined by their distance relative to the center of the phantom: (R1) 0-30mm, (R2) 30-43mm, and (R3) 43-65mm. In addition, a measure of through plane distortion was assessed by measuring the volume of signal void on a central image slice in all FSE and MAVRIC series and subtracting the known dimensions of the sample material. Statistics: One-way ANOVAs were performed to detect differences of overall mean displacement between the material samples and to detect differences of displacements between the 3 regions for each material sample. Statistical significance was set at $p < 0.05$. A post-hoc Student-Neuman-Keuls test was performed when significance was found. Measurement repeatability was assessed using Bland-Altman analysis.

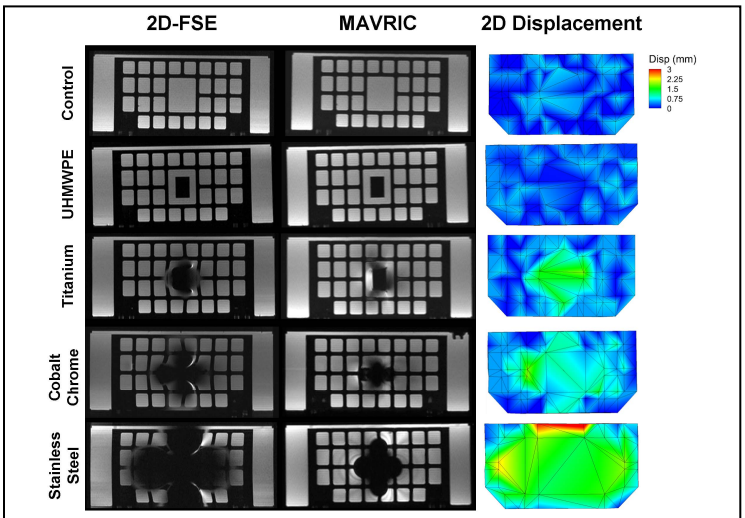

Figure 1. Representative 2D FSE images (Left), corresponding MAVRIC images (Center), and calculated in-plane displacement maps for grid corners between the FSE and MAVRIC image sets (Right).

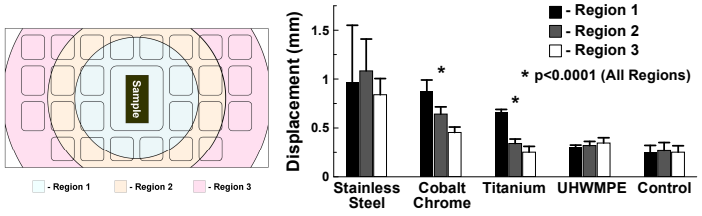

Figure 2. Left – Regions of analysis overlaid on the phantom grid. Right –Mean (± std.dev.) of image distortion of materials in each region between FSE and MAVRIC scans.

Results. Metal samples in the phantom produced visible distortions in 2D-FSE images and the distortions were reduced in MAVRIC images (Fig.1). Stainless Steel produced significantly more overall distortion than all other scans, Cobalt Chrome also produced significantly more overall distortion than all other scans. Titanium had more distortion than the UHMWPE and Control scans, and the distortion of the UHMWPE and the Control scans were similar to each other, $p<0.0001$. *Stainless Steel*: The mean (±std dev.) of all displacements between the FSE and MAVRIC series was 0.91±0.68 mm, with a median of 0.72mm. All subregions had similar levels of distortion, $p=0.5$ (Fig. 2). *Cobalt Chrome*: The average of displacements was 0.62±0.45 mm, with a median of 0.47mm . Region 1 had significantly more distortion than Regions 2 and 3, and Region 2 had significantly more distortion than Region 3, $p<0.0001$. *Titanium*: The average of displacements was 0.40±0.40mm, with a median of 0.47mm. Region 1 had significantly more distortion than Regions 2 and 3, and Region 2 had significantly more distortion than Region 3, $p<0.0001$. *UHMWPE*: The average of all displacements was 0.32±0.22mm, with a median of 0.37mm. All regions had similar distortions present, $p=0.12$. *Control*: The average of all displacements was 0.26±0.28mm, with a median of 0mm. All regions had similar distortions present, $p=0.8$. MAVRIC reduced the signal void by 53.4% for Stainless Steel, 71.1% for Cobalt Chrome, 19.1% for Titanium, and 4.8% for UHWMWPE. The repeatability of the measurements ranged from 0.51mm to 0.64mm across all material samples.

Discussion. The metal test samples produced the largest distortion fields. The distortions from the metals tended to be largest in Region 1, closest to the sample (Fig 2.). The Stainless Steel produced a distortion larger than Cobalt Chrome and Titanium; however, the distortion calculation for Stainless Steel in Region 1 may be underestimated due a limited number of data points being available. The distortion of the UHWMWPE, sub-pixel in magnitude, was similar to the Control scan, indicating that UHMWPE produces little to no distortions other than the baseline measurement noise of the system. The repeatability was approximately $\sqrt{2} \cdot$ pixel dimension, signifying the limited effects of voxel averaging and image post-processing between identical scans. MAVRIC scans also reduced through plane image distortion, as indicated by the reduction of size of signal void. The magnitude of through-plane distortions in conventional 2D-FSE images can be far greater than that of the in-plane distortions. Future studies will use the novel phantom to develop additional distortion quantitation techniques, including combined through-plane and in-plane distortions. **References**. 1. Koch KM et al., Magn Reson Med (61), 2009. 2. Koch KM et al, Magn Reson Med (65), 2011. **Acknowledgements**. Institutional research support was provided by General Electric Healthcare.